Light Confinement by a Cylindric Metallic Waveguide in Dense Buffer Gas Environment

Ulrich Vogl,* Anne Saß, Frank Vewinger, and Martin Weitz
Institut für Angewandte Physik der Universität Bonn, Wegelerstr. 8, D-53115 Bonn, Germany

Alexander Solovev, Yongfeng Mei, and Oliver Schmidt
Institute for Integrative Nanosciences, IFW Dresden, Helmholtzstr. 20, D-01069 Dresden, Germany

(Dated: December 8, 2010)

We report on the implementation of metallic microtubes in a system of rubidium vapour at 230 bar of argon buffer gas. The high buffer gas pressure leads to a widely pressure broadened linewidth of several nanometers, interpolating between the sharp atomic physics spectra and the band structure of solid state systems. Tube-like metallic waveguide structures have been inserted in the high pressure buffer gas system, allowing for an enhancement of the atom-light interaction over an optical guiding length in the tube of up to 1 mm. The system holds promise for nonlinear optics experiments and the study of atom-light polariton condensation.

PACS numbers: 32.80.-t, 05.30.Jp, 32.70.Jz, 42.50.Fx, 42.82.Et, 78.67.Ch

Confinement of optical radiation is a key prerequisite in experiments investigating Bose-Einstein condensation of polaritons. It allows to tailor the dispersion relation for this quasi-particles and enhances the obtainable matter-light interaction. Experimentally, exciton-polariton systems in microcavity structures gave evidence of quasiparticle condensation [1–3]. In a recent experiment, thermalization [4], and subsequently Bose-Einstein condensation [5] of a photon gas in a dye-filled optical microcavity has been observed, which emphasizes the capacity of this general approach.

A successful system for light confinement are e.g. hollow core fibers, which in principle allow strong light-matter coupling over long distances in a defined volume with a well defined intensity distribution [6–9]. The enhanced interaction in such systems has proven advantageous for electromagnetically induced transparency and four-wave-mixing [10, 11] with alkali vapour inside the fiber. This approach requires careful procedures to coat the inside of the fiber with certain carbon hydrides to avoid chemical adsorption of the alkali atoms to the silica bulk of the fiber and is thus not applicable for hot vapour.

In this paper we investigate light confinement using metal waveguides in a system of hot rubidium vapour and 200 bar of argon buffer gas pressure. The frequent collisions of the rubidium atoms with the buffer gas give a pressure broadened linewidth of a few nanometers, approaching the thermal energy k_BT of the system in wavelength units. We have shown recently that the frequent collisions with the buffer gas atoms can lead to thermal equilibrium of dressed states, i.e. coupled atom-light states [12, 13]. Another interesting possibility in this system are novel laser cooling schemes [14], which in a thermodynamic sense may also be seen as a consequence of coupling internal and external atomic degrees of freedom in the pressure broadened system. The nanosecond lifetimes of alkali excited states in high pressure buffer gas ($\tau_{nat} \simeq 27$ ns for the case of the 5P state of the rubidium atom) is orders of magnitude longer than the picoseconds relaxation times of typical exciton-polariton systems. Thus, there are prospects that atomic physics based polariton condensation experiments can achieve longer coherence times than exciton polariton systems. On the other hand, the high required temperatures of the rubidium-high pressure buffer gas system (350°C are required to reach 1 mbar Rb vapour pressure, which is the typical equivalent to an optically dense buffer gas broadened system) make it experimentally challenging to implement the required optical resonator or waveguide structures for a particle-like tailoring of the dispersion relation in the alkali vapour environment. Standard quartz-based optical fiber structures or mirrors are known to adsorb alkali vapour at temperatures above 150-200°C. Similarly, organic protective coatings become unstable at the used high temperatures. An interesting alternative possibility is the use of metallic microstructures, which have higher chemical stability under the here present conditions. Novel manufacturing techniques have recently allowed for the fabrication of ultra thin, rolled metal tubes that can suit the mentioned preconditions [15].

In this work we report on the implementation of metallic microtubes into a system of rubidium atoms at 230 bar argon buffer gas pressure. The ultra thin microscopic (6 μm diameter) metal structures allow to guide light over a distance of 1 mm in the high pressure buffer gas environment. The light traversing the metal tubes shows an increased Stokes shifted part of the spectrum with respect to free propagation in the cell, which is attributed to the enhanced atom-light interaction achieved by the light confinement in the waveguide.

Let us begin by discussing a few general features of the used metallic microtube structures. Such microstruc-

tures can be engineered with high precision by depositing, releasing and rolling up thin metallic membranes [15, 16]. The fabrication process of these tubes allows for a wide variety of diameters from nanometer to several micrometer and a length up to a few millimeter, resulting in aspect ratios of up to 1:10000. The technique is applicable to a variety of materials including combinations of semiconductors, metals and oxides [17]. Figure 1a shows a Scanning Electron Microscopy (SEM) image of a rolled up microtube fabricated on silicon substrates by underetching of photoresist sacrificial layer. The prepared microtube consists of Ni/Fe/Ag layers and has an internal diameter of $6\pm0.3\,\mu$m. Figure 1b shows a SEM image of a microtube transported onto a metallic holder for the integration into the optical setup. The inset of Figure 1b indicates sandwiched Ni/Fe/Ag rolled up layers. A general description for the production of these waveguides can be found in [16], for the here used samples we applied the following steps: The Ni/Fe/Ag microtubes were fabricated by electron-beam deposition of metals onto lithographically patterned photoresist layers. Square AR-P 3510 photoresist patterns with the length of 1 mm were prepared on 1.5-inch silicon wafer. Photoresist was spin-coated at 3500 rpm for 35 s, followed by a soft bake using a hotplate at 90°C degrees for 1 minute and exposure to UV light with a Karl Suss MA56 Mask Aligner (410-605 nm). Patterns were developed in a 1:1 AR300-35:H2O. Ni/Fe/Ag layers were deposited with corresponding thicknesses 20/20/20 nm on the sample tilted to 65° from the horizontal line. The tubes were then rolled up by underetching of the sacrificial photoresist layer in acetone followed by rinsing in isopropanol. The samples were transferred into the supercritical point dryer to avoid the tube collapsing due to the high capillary pressure (surface tension) of the evaporated solvents. After drying the microtubes were released using glass micro-capillary and transferred on the metallic holder. The fabricated structures are then mounted within the high pressure environment.

In previous experiments [12] we used a freely propagating laser beam, which was tightly focused to a beam waist of $w_0 = 6\,\mu$m and directed into the vapour cell. The region of fairly high and uniform intensity is then limited to twice the Rayleigh length $2z_R = \frac{2\pi\omega_0^2}{\lambda} = 70\,\mu$m, with the typical used wavelength of 800 nm. Confinement in a metallic tube over a distance up to 1 mm thus can enhance the effective interaction length by more than an order of magnitude. A drawback of metallic waveguides is their relatively large loss compared to dielectric waveguides, which is due to resistive losses in the metal. Compared to massive metallic structures thin-walled structures with wall thickness of order of the skin-depth can in principle lead to an enhanced transmission [18, 19]. A further notable benefit of such metal structures is that light confinement to diameters below the size of the wavelength can be achieved, an issue that has allowed for extraordinarily high transmission through subwavelength diameter holes [20]. In an interesting experiment with a planar configuration with similar sub-wavelength silver layers the strong coupling regime could be realized [21]. The silver layers in this experiment formed a low-Q cavity and the strong coupling could be realized with the metal boundary condition providing a stronger confinement than dielectric cavity mirrors.

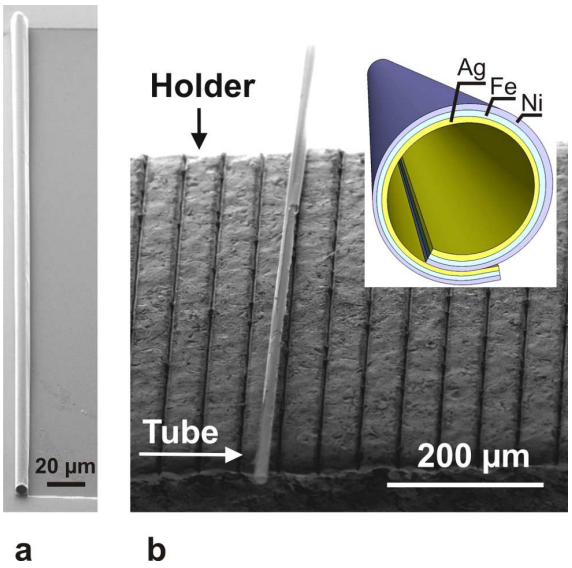

FIG. 1: Single metallic microtube. (a) Scanning electron microscope (SEM) image of a rolled up metallic microtube on silicon substrate. (b) The microtube attached to a metallic holder for the integration into the optical setup.

In the present work we use a diameter of the waveguide of $6\,\mu$m, which is several times the wavelength of the used radiation ($\lambda \sim$800 nm, tuned near the rubidium D-lines). The wall thickness is 60 nm, consisting of Ni/Fe/Ag layers, 20 nm each. This is still in the order of magnitude of the estimated skin depth of the structure (the skin depth of the inner silver layer is approximately 12 nm for the used wavelength and the thickness of the layer [22]). Our experimental apparatus is shown in Figure 2. A steel chamber with sapphire optical windows is heated to 550 K, yielding 1 mbar rubidium vapour pressure (number density $10^{16}\,\mathrm{cm}^{-3}$) and 230 bar argon buffer gas pressure. The metallic waveguide (Figure 1) is placed on a holder inside the cell, facing the entrance window of the cell. Tunable laser radiation from a cw-Titanium-Sapphire laser is directed via a confocal beam geometry to a movable achromatic lens system and then focused into the cell. This setup allows to monitor the location of the laser focus with a control pinhole and simultaneously steer the microtubes to the focal point of the objective. The transmitted light was collected and detected spectrally resolved.

Let us begin discussing experimental data by showing a

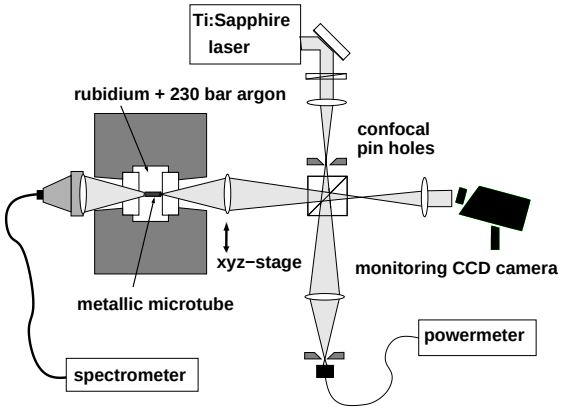

FIG. 2: Experimental setup. With a confocal geometry the position of the laser focus is monitored at a pinhole. A translation stage at the objective allows for lateral scan of the focus position relative to the microtube.

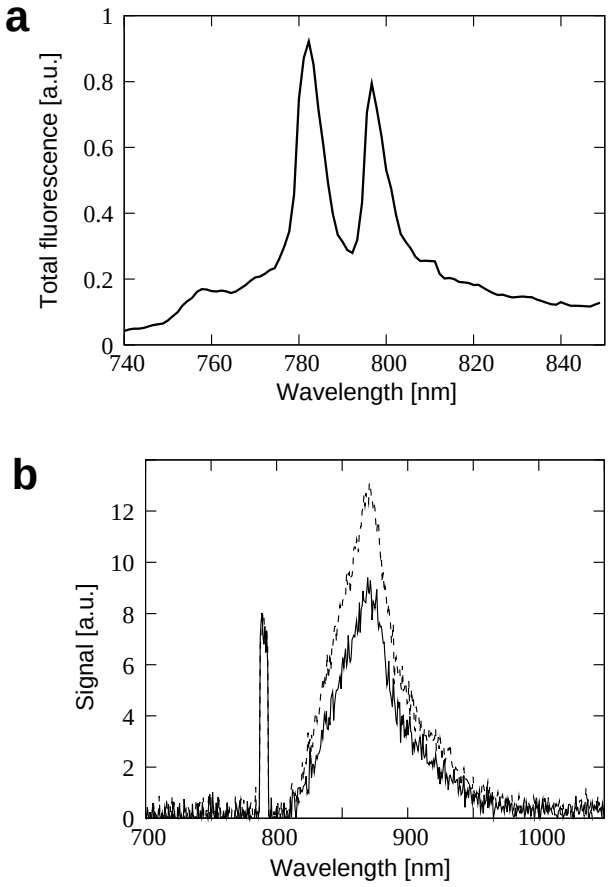

FIG. 3: (a) Spectrum of rubidium with 230 bar argon buffer gas, recorded in backwards direction. The main features are the two fine structure transitions at 780 and 795 nm (Rb D2 and D1 lines respectively). The whole spectrum is strongly pressure broadened. (b) Typical spectra of the radiation detected after the cell versus wavelength for an incident wavelength of 785 nm. One observes a sharp carrier, which is the remainder of the exciting laser, and a broad Stokes-scattered band between 825 and 950 nm. The solid line shows a spectrum for free transmission. An enhanced Stokes-band is obtained when the interaction length is increased by transmission through the tube (dashed line).

typical spectrum in the high pressure buffer gas environment recorded in backwards direction (shown in Fig. 3a), where the pressure broadened rubidium D1 and D2-line resonances are clearly visible. The observed linewidth (FWHM) is roughly 3 nm at the used buffer gas pressure of 230 bar. The spectral width here approaches the thermal energy in the heated gas cell ($k_BT \approx 20$ nm in wavelength units at the D-lines wavelengths and 550 K temperature) within an order of magnitude. It is well known that in strongly pressure broadened systems redistribution of the atomic fluorescence can occur [23]. In earlier work we observed that the frequent collisions combined with an excited state lifetime that exceeds the typical collision time by three orders of magnitude leads to a complete redistribution of fluorescence, yielding a spectrum centered around the two fine structure lines at 780 nm and 795 nm in this system [14].

To investigate the possible influence of the microtubes we analyzed the light in forward direction. A typical corresponding spectrum of the transmitted light after the cell without metal tube is shown by the solid line in Fig. 3b. The used laser wavelength here was near 785 nm, i.e. in the vicinity of the rubidium D-lines, and the visible sharp peak in the spectrum at the incident wavelength is due to remaining transmitted radiation at the carrier wavelength. The used optical density is about 3 at the incident laser wavelength, and most of the fluorescence is multiply reabsorbed and scattered spatially into the full solid angle and spectrally to the far wings of the fluorescence spectrum. A main feature of the measured spectra is a relatively strong and spectrally broad band between 825 and 950 nm.

Scattered radiation that is closer to resonance within the observed spectrum is suppressed, as can be understood by the stronger absorption for near-resonant light, leading to the observed radiation at the end of the cell (apart from a remaining part of the incident laser frequency peak) mainly being far red-shifted radiation. We attribute the observed red-shifted spectral components in Fig. 3b to be mainly due to emission from Rubidium-Argon excimer states [24], comparable to similar features in Rb-He exciplexes [25, 26]. Its origin are optical collisions with large energy exchange, that result in a spectral shift of the fluorescence photons into the transparent region of the vapour.

As the end of the metal tube is otherwise poorly accessible within the cell, we use this red shifted spectral band as an indicator for the influence of the metal tube. To place the microtubes controlled into the optical path we initially matched the position of the tube ending and the focus of the laser beam with the confocal setup shown in Figure 2. By a lateral scan of the laser beam over the end

face of the metal tube we could clearly identify the tube walls as a sharp drop of the total transmission power. For the subsequent measurements we aligned the laser beam to the so determined center of the end face of the metal tube. The used laser power in these and the following measurements was 1 W. By monitoring the metal tube no degradation was observed despite the relatively high light intensity at the tube entrance of $10^7\,\mathrm{W/cm^2}$. The so obtained spectra show an enhanced intensity in the Stokes-band compared to the free transmission situation, as it is exemplified shown in Fig. 3b. The spectrum with the tube inserted is indicated with the dashed line and compared to the free transmission case (solid line) shows with otherwise same conditions a clearly enhanced Stokes band.

Datasets as shown in Figure 3b were taken for various incident laser wavelengths in the range between 750-830 nm, both again with the laser beam aligned to the microtube and for comparison with free running laser beam. The difference between the aligned and free running case show a pronounced wavelength dependence. To compare the two cases and to reduce systematics we obtained the ratio of the transmitted light power in the carrier and the Stokes band for transmission through the microtube and for free transmission. The result of a corresponding measurement is shown in Fig. 4 versus the incident laser wavelength. While far from the rubidium D-lines there is no significant difference observed between free space propagation, in the spectral range between 785 and 800 nm (roughly in between the D-lines) one observes an enhanced transfer into the Stokes-shifted infra-red band. One also observes some decrease of the transfer near laser wavelengths of 778 nm and 802 nm. The absolute detected power integrated over the whole spectral range is determined to be attenuated by a factor 1.3 when the laser is directed at the microtube, but the optical power in the spectral range of the Stokes band is strongly enhanced at an incident laser wavelength of 795 nm, indicating enhanced atom-light interaction due to the confinement of the metallic microtube. A straightforward explanation for this behaviour is that a part of the light that is scattered and spectrally redistributed by the rubidium atoms is guided by internal reflection through the microtube. In earlier work we have observed that an increased optical intensity leads to a larger linewidth of the pressure broadened line, as can be understood by saturation broadening. The here used confinement over a longer distance than the Gaussian beam focus thus is expected to enhance the atom-light interaction of the incident laser beam. We observe such an enhancement when the excitation wavelength is tuned in between of the rubidium D-lines. In this near-resonant spectral region the vapour is relatively optical dense and multiple reabsorption of photons can be expected. While for a free running laser beam the diffusion of multiply reabsorbed light leads to strong losses along the beam direction, here reflection at

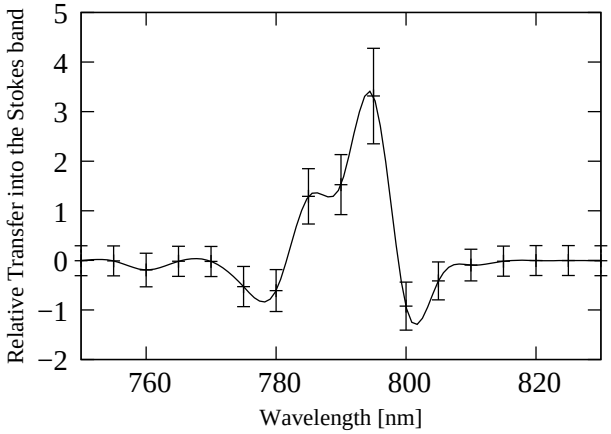

FIG. 4: Ratio between the light power transferred into the Stokes-band and the carrier transmission intensity for different excitation wavelengths. The plot shows the the relative deviation of the transfer into the Stokes band compared to the case of free transmission, given by $I^{\mathrm{tube}}_{\mathrm{Stokes}}/I^{\mathrm{tube}}_{\mathrm{Carrier}} - I^{\mathrm{free}}_{\mathrm{Stokes}}/I^{\mathrm{free}}_{\mathrm{Carrier}}$ We estimate a statistical error of 10%. An enhanced transfer into the Stokes-band is obtained in the spectral region between the D1 and D2 line.

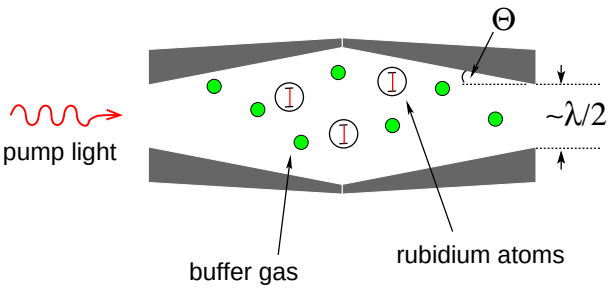

FIG. 5: Proposed biconical waveguide design with cut-off within the redistributed fluorescence spectrum of rubidium. The system can be optically pumped with short-wavelength light exciting the pressure broadened rubidium resonances. Subsequent redistribution of fluorescence towards longer wavelength can accumulate photons near the cut-off of the waveguide. The diameter of the structure should be in the order of $\lambda/2$ of the used laser wavelength. A nonvanishing inner cone angle Θ of the biconical structure allows for the tailoring of the allowed modes inside the cavity [27], and provides a trapping potential along the weakly confined axis.

the silver coated tube walls favours scattering along the tube axis. We note that further contribution to the enhanced intensity of the Stokes shifted fluorescence could be due to internal reflection and surface effects at the silver coated tube.

This first results with a cylindrical waveguide with relatively large diameter are encouraging for further actions towards light confinement within the waveguide and in the long run polariton condensation with the waveguide modifying the the dispersion relation, and possibly also acting as a trapping potential. The combined system of thin-walled metallic waveguides with rubidium vapour in

a high buffer gas environment exhibits several qualities that make it a promising candidate for further investigations. The frequent collisions of rubidium atoms with noble gas atoms under optical radiation can drive coupled atom-light states towards thermal equilibrium. This can be further supported by the enhanced interaction within the waveguide. For the future, the waveguides which have now been designed cylindrical with relatively large diameter can be tailored to smaller diameters, which increases the confinement. In particular, for a diameter of order of $\lambda/2$, the cut-off wavelength will reach within the redistributed fluorescence spectrum, similarily as in [4]. In this regime we expect that photons - or, when the strong coupling regime is reached, atom light polaritons - thermalize above the cavity cut-off, i.e. their frequencies will be distributed by an amount k_B/T above the cut-off frequency. The strong transverse confinement makes the system effectively one-dimensional. Furthermore, by using a biconical design as indicated in Fig. 5 a trapping potential can be realized, that in first order is of the form $V(z) \propto |z|$, where z is the direction along the symmetric axis (in analogy to [4]). This linearly confined, one-dimensional system is expected to support a BEC in the ideal gas case at sufficiently low temperatures and high densities (the general requirement is that the trapping potential here should be more confining than parabolic [28]). A detection of the optical radiation could be realized e.g. by collection of the light leaking out through one of the apertures, or for a tube with ultrathin walls by light leaking at the waist of the waveguide.

To conclude, we have shown that metallic microtubes can be integrated in a high pressure buffer gas optical spectroscopy setup. The material properties allow investigations in experimental regimes that are not easily accessible with comparable structures based on silica. Due to the high thermal conductivity of the metal and the surrounding argon gas, light intensities of up to $10^7\,\mathrm{W/cm^2}$ have been applied without thermal degradation. These highly versatile structures could pave the way to new approaches in the strong coupling between light and matter, or more specific for the investigation of collective atom-light states. Further investigations will include the study of smaller structures and waveguides with broken axial symmetry.

Financial support from the DFG within the focused research unit FOR557 and under the cooperation project 436RUS113/996/0-1 is acknowledged. The authors acknowledge helpful discussions with A. P. Alodjants and I. Y. Chestnov.

* Electronic address: vogl@iap.uni-bonn.de

[1] J. Kasprzak, M. Richard, S. Kundermann, A. Baas, P. Jeambrun, J. M. J. Keeling, F. M. Marchetti, M. H. Szymanska, R. Andre, J. L. Staehli, V. Savona, P. B. Littlewood, B. Deveaud and L. S. Dang. *Bose-Einstein condensation of exciton polaritons*. Nature **443**, 409 (2006).

[2] C. W. Lai, N. Y. Kim, S. Utsunomiya, G. Roumpos, H. Deng, M. D. Fraser, T. Byrnes, P. Recher, N. Kumada, T. Fujisawa and Y. Yamamoto. *Coherent zero-state and π-state in an exciton-polariton condensate array*. Nature (London) **450**, 529 (2007).

[3] A. Amo, J. Lefrère, S. Pigeon, C. Adrados, C. Ciuti, I. Carusotto, R. Houdré, E. Giacobino and A. Bramati. *Superfluidity of polaritons in semiconductor microcavities*. Nature Physics **5**, 805 (2009).

[4] J. Klaers, F. Vewinger and M. Weitz. *Thermalisation of a two-dimensional photonic gas in a white-wall photon box*. Nature Physics **6**, 512 (2010).

[5] J. Klaers, J. Schmitt, F. Vewinger and M. Weitz. *BoseEinstein condensation of photons in an optical microcavity*. Nature in press (doi:10.1038/nature09567) (2010).

[6] R. F. Cregan, B. J. Mangan, J. C. Knight, T. A. Birks, P. S. J. Russell, P. J. Roberts and D. C. Allan. *Single-Mode Photonic Band Gap Guidance of Light in Air*. Science **285**, 1537 (1999).

[7] S. Ghosh, J. E. Sharping, D. G. Ouzounov and A. L. Gaeta. *Resonant Optical Interactions with Molecules Confined in Photonic Band-Gap Fibers*. Physical Review Letters **94**, 093902 (2005).

[8] M.-L. Hu, C.-Y. Wang, Y.-J. Song, Y.-F. Li, L. Chai, E. E. Serebryannikov and A. M. Zheltikov. *A hollow beam from a holey fiber*. Optics Express **14**, 4128 (2006).

[9] M. Bajcsy, S. Hofferberth, V. Balic, T. Peyronel, M. Hafezi, A. S. Zibrov, V. Vuletic and M. D. Lukin. *Efficient All-Optical Switching Using Slow Light within a Hollow Fiber*. Physical Review Letters **102**, 203902 (2009).

[10] F. Benabid, F. Couny, J. C. Knight, T. A. Birks and P. S. J. Russell. *Compact, stable and efficient all-fibre gas cells using hollow-core photonic crystal fibres*. Nature (London) **434**, 488 (2005).

[11] P. Londero, V. Venkataraman, A. R. Bhagwat, A. D. Slepkov and A. L. Gaeta. *Ultralow-Power Four-Wave Mixing with Rb in a Hollow-Core Photonic Band-Gap Fiber*. Physical Review Letters **103**, 043602 (2009).

[12] U. Vogl and M. Weitz. *Spectroscopy of atomic rubidium at 500-bar buffer gas pressure: Approaching the thermal equilibrium of dressed atom-light states*. Phys. Rev. A **78**, 011401 (2008).

[13] I. Y. Chestnov, A. P. Alodjants, S. M. Arakelian, J. Nipper, U. Vogl, F. Vewinger and M. Weitz. *Thermalization of coupled atom-light states in the presence of optical collisions*. Phys. Rev. A **81**, 053843 (2010).

[14] U. Vogl and M. Weitz. *Laser Cooling by Collisional Redistribution of Radiation*. Nature, London **461**, 70 (2009).

[15] A. Solovev, Y. Mei, E. Bermúdez Ureña, G. Huang and O. G. Schmidt. *Catalytic Microtubular Jet Engines Self-Propelled by Accumulated Gas Bubbles*. Small **5**, 1688 (2009).

[16] Y. Mei, G. Huang, A. A. Solovev, E. Bermúdez Ureña, I. Mönch, F. Ding, T. Reindl, R. K. Y. Fu, P. K. Chu and O. G. Schmidt. *Versatile Approach for Integrative and Functionalized Tubes by Strain Engineering of Nanomembranes on Polymers*. Advanced Materials **20**, 4085 (2008).

[17] O. G. Schmidt and K. Eberl. *Nanotechnology: Thin solid*

films roll up into nanotubes. Nature (London) **410**, 168 (2001).

[18] J. Takahara, S. Yamagishi, H. Taki, A. Morimoto and T. Kobayashi. *Guiding of a one-dimensional optical beam with nanometer diameter*. Optics Letters **22**, 475 (1997).

[19] H. F. Ghaemi, T. Thio, D. E. Grupp, T. W. Ebbesen and H. J. Lezec. *Surface plasmons enhance optical transmission through subwavelength holes*. Phys. Rev. B **58**, 6779 (1998).

[20] J. Rybczynski, K. Kempa, A. Herczynski, Y. Wang, M. J. Naughton, Z. F. Ren, Z. P. Huang, D. Cai and M. Giersig. *Subwavelength waveguide for visible light*. Applied Physics Letters **90**, 021104 (2007).

[21] P. A. Hobson, W. L. Barnes, D. G. Lidzey, G. A. Gehring, D. M. Whittaker, M. S. Skolnick and S. Walker. *Strong exciton-photon coupling in a low-Q all-metal mirror microcavity*. Applied Physics Letters **81**, 3519 (2002).

[22] Z. Wang, X. Cai, Q. Chen and L. Li. *Optical properties of metal-dielectric multilayers in the near UV region*. Vacuum **80**, 438 (2006).

[23] C. Cohen-Tannoudji, J. Dupont-Roc and G. Grynberg. *Atom-Photon Interactions - Basic Processes and Applications* (Wiley, New York, 1992).

[24] J. Pascale and J. Vandeplanque. *Excited molecular terms of the alkali-rare gas atom pairs*. J. Chem. Phys. **60**, 2278 (1974).

[25] K. Hirano, K. Enomoto, M. Kumakura, Y. Takahashi and T. Yabuzaki. *Emission spectra of Rb^*He_n exciplexes in a cold ^4He gas*. Phys. Rev. A **68**, 012722 (2003).

[26] J. F. Sell, M. A. Gearba, B. M. Patterson, T. Genda, B. Naumann and R. J. Knize. *Enhancement of Rb fine-structure transfer in 4He due to three-body collisions*. Opt. Lett. **35**, 2146 (2010).

[27] V. Kravchenko, V. Veretel'nik and V. L. Rvachev. *Calculation of electrodynamic properties of a biconical resonator*. Measurement Techniques **36**, 337 (1993).

[28] V. Bagnato and D. Kleppner. *Bose-Einstein condensation in low-dimensional traps*. Phys. Rev. A **44**, 7439 (1991).